Journal of Physics: Conference Series **568** (2014) 022011 doi:10.1088/1742-6596/568/2/022011

Influence of thermal gradient in vortex states of mesoscopic superconductors

E C S Duarte[1], A Presotto[1], D Okimoto[1], E Sardella[2,3], R Zadorosny[1]

[1] Departamento de Física e Química, Univ Estadual Paulista - Unesp, Ilha Solteira, SP, Brazil, CEP 15385-000

[2] UNESP-Universidade Estadual Paulista, Faculdade de Ciências, Departamento de Física, CEP 17033-360, Bauru-SP, Brazil

[3] UNESP-Universidade Estadual Paulista, IPMet-Instituto de Pesquisas Meteorológicas, CEP 17048-699, Bauru-SP, Brazil

E-mail: elwis.gapira@gmail.com

Abstract.

In general, the studies of finite size effects in mesoscopic superconductors have been carried out in such a way that the temperature parameter is constant in the entire system. However, we could have situations where a real sample is near a heater source, as an example. In such situations, gradients of temperature are present. On the other hand, mesoscopic superconductors are interesting systems due to the fact that they present confinement effects which influence all the vortex dynamics. Thus, in this work we studied the influence of thermal gradients on the vortex dynamics in mesoscopic superconductors. For this purposes, we used the time dependent Ginzburg-Landau equations. The thermal gradients produce an asymmetric distribution of the currents around the system which, in turn, yield interesting vortex configurations and difficult the formation of giant vortices.

1. Introduction

The time dependent Ginzburg-Landau (TDGL) theory has been successfully used in the last decades to describe several aspects of mesoscopic superconducting systems. Such systems present small size of the order of penetration depth $\lambda(T)$ and/or the coherence length $\xi(T)$, where T is the temperature. By using the TDGL formalism, several works have demonstrated that the confinement effects induce the formation of multi-vortex (MV) and giant vortex (GV) states [1]-[4]. This depend of the temperature and the system geometry [5]-[11]. Also, the presence of surface defects and De Gennes boundary conditions modify the vortex dynamics of mesoscopic systems [12], in such way that differs from the dynamics presented by the macroscopic ones [13]-[14]. In this work, we study the behavior of the vortex dynamics in mesoscopic systems in the presence of linear thermal gradients. Then, we analyze their magnetic properties, the vortex configurations, and the possible formation of a GV state.

2. Theoretical formalism

The formalism which we used was firstly proposed by Schimid[15], and it is a generalization of the Ginzburg-Landau (GL) equations, where a temporal evolution of the order parameter ψ

Content from this work may be used under the terms of the Creative Commons Attribution 3.0 licence. Any further distribution of this work must maintain attribution to the author(s) and the title of the work, journal citation and DOI.
Published under licence by IOP Publishing Ltd

and the potential vector $\mathbf{A}$ was inserted; $|\psi|^2$ is the density of superelectrons and the induction magnet field is given by $\mathbf{B} = \nabla \times \mathbf{A}$. In dimensionless units, the TDGL equations are given by

$$\frac{\partial \psi}{\partial t} + \imath\varphi\psi = (-i\boldsymbol{\nabla} - \mathbf{A})^2\psi + \psi(1 - T(x) - |\psi|^2) \, , \tag{1}$$

$$\beta\frac{\partial \mathbf{A}}{\partial t} + \boldsymbol{\nabla}\varphi = \mathbf{J_S} - \kappa^2\boldsymbol{\nabla} \times \boldsymbol{\nabla} \times \mathbf{A} \, , \tag{2}$$

where de superconductivity current density is given by

$$\mathbf{J_S} = \mathrm{Re}(\psi^*(-\imath\nabla - \mathbf{A})\psi) \, . \tag{3}$$

For the thermal gradient we assumed a linear dependence of T along the x axis which is given by

$$T(x) = T_l + \frac{T_r - T_l}{a}x \, , \tag{4}$$

where T_r and T_l are the temperatures at the right-hand (hottest) and left-hand (coldest) side of the superconducting square. All equations have been normalized. The distances are in units of the coherence length $\xi(0)$; the magnetic field in units of the bulk upper critical field $H_{c2}(0)$ and the temperature in units of the critical temperature T_c; $\kappa = \lambda(T)/\xi(T)$ is the GL parameter. The TDGL equations are gauge invariant under the transformations: $\psi' = \psi e^{i\chi}$, $\mathbf{A'} = \mathbf{A} + \nabla\chi$, $\varphi' = \varphi - \frac{\partial\chi}{\partial t}$. We have worked in the Coulomb gauge where $\varphi' = 0$ for all times and positions. We numerically solved such equations by using the link variable method [16]. This method is preferably used because it preserves the gauge invariance of the equations once they are discretized. The TDGL equations will be used only as a relaxation method to obtain the steady state, that is, we are solely interested in the equilibrium vortex configurations.

3. Results and Discussion

We carried out the numerical simulations considering square systems with lateral size of $12\xi(0)$ and GL parameter $\kappa = 5$, which is equivalent to a Pb-In alloy[17]. We also used the following simulation parameters: $\beta = 1$; the size of the mesh was taken as $\Delta x = \Delta y = 0.125\xi(0)$ and the steps of the external magnetic field $\Delta H = 10^{-3}$. All the dynamics were analyzed under a thermal gradient which changes the value of ψ along the x axis of the system. In this work, we investigated the dynamics of two systems under two different thermal gradients, i.e, one in which the temperature varies from $0.7T_c$ to $0.9T_c$, label by S_1 and another one from $0.8T_c$ to $0.85T_c$, labeled by S_2. We also compared the results with a system at a homogeneous temperature (HT for brief) distribution by taking $T = 0.85T_c$. In Fig. 1 we present the magnetization curve as a function of the applied magnetic field of the systems under investigation. The behavior of such curves are similar to those ones exhibited by the HT systems, i.e., each discontinuity is due to one or more vortex penetration. Note that, the field corresponding to the first penetration for the S_1 system is lower than for the S_2 one. This is due to the fact that S_1 has its right-hand side hotter than S_2 which, on its turn, has a similar behavior presented by the HT system. The field sufficient for the destruction of superconductivity is higher for S_1 than for S_2 because temperature in the colder region is lower for the former system. In Fig. 2 we illustrate the profile of the modulus the current density, J/J_0, where J_0 is the despairing current, along the x axis and for three different distances w from the bottom side of the system (see inset of Fig. 1). A comparison between S_1 and S_2 is showed in Fig. 2. It is worth noticing the asymmetric distribution of J in comparison with the inset of this same figure for the HT system. However, S_2 presents a less asymmetric profile when it is compared with S_1. Also, it can be observed that J presents a higher value in the colder region and a degradation of superconductivity in the hottest one. We notice that with both perturbations S_1 and S_2 the vortices nucleate inside

the superconductor one by one. As expected, the penetration always occurs at the right-hand side of the system.

We also studied the influence of non-homogeneous distribution of temperature on the giant vortex state which has been found for the HT systems [18]. In Fig. 3 we show two vortex state for S_1, S_2 and HT. In the panel 3(a) it is shown the intensity of $|\psi|$ superimposed by the streamlines **J**. In such figure is clearly seen two separate vortices which is confirmed by the phase of ψ in panel 3(b). The other hand, the equivalent panels 3(c) and (d) for S_2, and 3(e) and (f) for the HT system, we clearly see the formation of giant vortex state. As a consequence, we can say that a rather non-homogeneous temperature like S_2 is not sufficient to avoid the nucleation of such state.

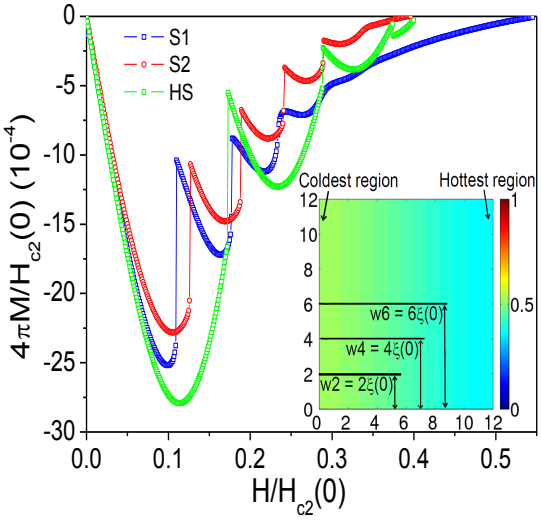

Figure 1. The magnetization curve as a function of the external applied field for the S_1, S_3 and HT systems. The inset shows the intensity of the order parameter in the initial state (without applied magnet field) under a thermal gradient.

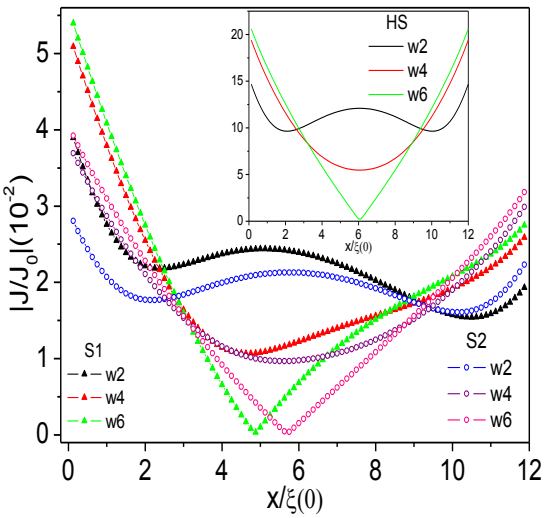

Figure 2. Profile of the modulus of the current along the x axis for three different levels of the square shown in the inset of Fig. 1 for S_1 and S_2. In the inset of the present figure it is shown the symmetric profile of the current for the HT system.

Fig. 4 illustrate the scenario associated with the third penetration. S_1 and S_2 present the same penetration dynamics with three nucleated vortices in the stationary state. However, the HT system presents four vortex state just after the third penetration (see panels 4(e) and (f)). This indicates that the thermal gradient breaks the fourfold symmetry of the multi-vortex state in those systems. On the other hand, it is interesting to note that giant vortex is created in S_1, which means that a greater variation of the temperature induces a non-conventional vortex interaction.

4. Conclusion

In this work we studied two systems with different thermal gradients by using the time dependent Ginzburg-Landau equations. It was shown that a variation of the temperature induces an asymmetric distribution of **J** along the system which is responsible for non-conventional behavior of the vortex dynamics. Depending on the conditions, such the range of variation of T and the number of penetrated vortices, giant vortex states can be avoided. Another interesting behavior is the break of the fourfold symmetric of the third penetration presented by the systems with thermal gradients in comparison with a system in a uniform temperature.

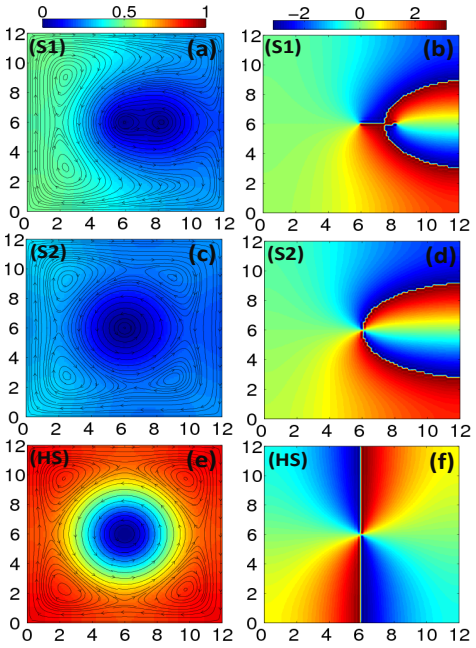

Figure 3. Left: intensity of the order parameter; right: phase of the order parameter; S_1 (a,b); S_2 (c,d); HT (e,f).

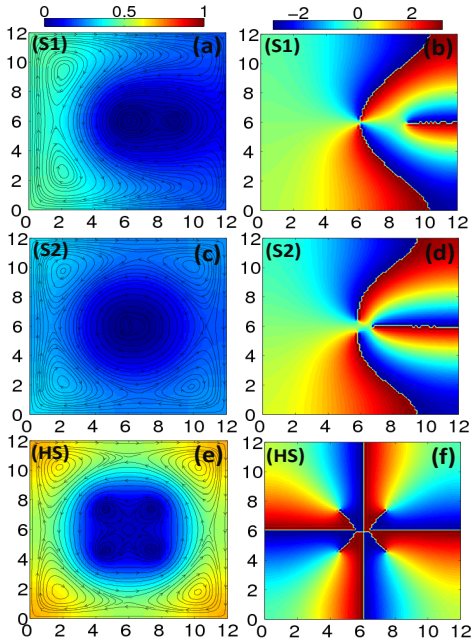

Figure 4. The same as for Fig. 3; S_1 (a,b); S_2 (c,d); HT (e,f).

5. Acknowledgments

We thank the Brazilian Agencies Fundunesp/PROPe grant 2115/002/14-PROPe/CDC and the São Paulo Research Foundation (FAPESP), grants 2013/17719-8 and 2012/04388-0 for financial support.

6. References

[1] Machida M, Kaburaki, H 1993 *Phys.Rev.Lett* **71** 3206–3209
[2] Bolech A C, Buscaglia G C, Lopez A, 1995 *Phys.Rev.B* **52** 15719–15722
[3] Deo P S, Schweigert V A, Peeters F M, Geim A K 1997 *Phys.Rev.Lett* **79** 4653–4657
[4] Schweigert V A, Peeters F M 1998 *Phys.Rev.B* **57** 13817
[5] Schweigert V A, Peeters F M 1999 *Phys.Rev.B* **60** 3084–3087
[6] Cren T, Garcia L S, Debontridder F, Roditchev D 2011 *Phys.Rev.Lett* **107** 097202
[7] Baelus B J, Kanda A, Peeters F M, Ootuka Y, Kadowaki K 2005 *Phys.Rev.B* **71** 140502
[8] Sardella E, Lisboa-Filho P N, Malvezzi A L 2008 *Phys.Rev.B* **77** 104508
[9] Presotto A, Sardella E, Zadorosny R 2013 *Physica C* **492** 75–79
[10] Palacios J J 1998 *Phys.Rev.B* **58** R5948-R5951
[11] Zadorosny R, Sardella E, Malvezzi A L, Lisboa-Filho P N, Ortiz W A 2012 *Phys.Rev.B* **85** 214511
[12] Barba-Ortega J, Gonzlez J D, Sardella E 2014 *J.Low.Temp.Phys* **174** 96–103
[13] Barba-Ortega J, Sardella E, Aguiar J A, Brant E H 2012 *Physica C* **479** 49–52
[14] Connolly M R, Milosevic M V, Bending S J, Clem J R, Tamegai T 2009 *Euro.Phys.Lett* **85** 17008
[15] Schimid A 1966 *Phys.Kondens.Materie* **5** 302–317
[16] Gropp W D, Kaper H G, Leaf G K, Levine D M, Palumbo M, Vinokur V M 1996 *J.Comput.Phys* **123** 254–266
[17] Poole Jr C P, Farach H A, Creswick R J, Prozorov Ruslan 2007 *Superconductivity* 2.ed (Amsterdam: Elsevier) p 670
[18] Sardella E, Malvezzi A L, Lisboa-Filho P N, Ortiz W A 2006 *Phys.Rev.B* **74** 014512